SMAR 2015 – Third Conference on Smart Monitoring,
Assessment and Rehabilitation of Civil Structures

Assessment of Defects in Cemented Materials Using Ultrasonic Waves

Ahmet Serhan Kırlangıç[1], Giovanni Cascante[2], and Maria Anna Polak[2]

[1] Cranfield University, Bedford, United Kingdom
[2] University of Waterloo, Waterloo, ON, Canada

ABSTRACT: An overall assessment procedure based on wave attenuation and dispersion of the phase velocity is proposed for the concrete structural elements with irregular defects. The attenuation is determined by utilizing discrete wavelet transform while the dispersion is extracted from two-dimensional Fourier transform. A new diagnostic feature, dispersion index, representing the cumulative variation in the phase velocity with respect to the reference dispersion curve obtained from the intact material is defined to evaluate the discrete defects in a quantitative manner. Investigations are initiated on a half-space medium of cemented-sand with regular-shaped defects first to establish the methodology. Then, a pilot study is conducted to evaluate the damage level of six laboratory-scale concrete beams with unevenly distributed defects. Despite the complex structure of the defect patterns and beam geometry, promising diagnostic features are obtained from both attenuation and dispersion based assessments.

1 INTRODUCTION

Deterioration in concrete structures may be caused by many reasons (e.g. corrosion, overloading, aging, temperature effects, ground shaking) that produce cracks either in micro or macro scale. Methods based on surface wave propagation have been used for evaluating the degradation in concrete. Monitoring variations in the wave characteristics, such as attenuation and dispersion, makes it possible to infer the material conditions. Previous studies utilizing the surface wave methods to detect the surface-breaking cracks provided satisfactory results (Yang et al. 2009, Yang et al. 2010, Zerwer et al. 2005, Zerwer et al. 2003, Popovics et al. 2000, Kalinski et al. 1999). In these studies, the crack is simulated by a notch to investigate localized defect instead of overall assessment of the element, which limits the practicability in the field applications as the test procedure has to be repeated for different cracks along the structural element. Distributed defects with different volume and orientation in materials were also studied in time and frequency domains by Aggelis et al. (2007, 2009a, 2009b). Nevertheless, the information extracted from the wave signals can be improved by using advanced signal processing techniques.

The objective of this paper is to establish an overall methodology for condition assessment of cemented materials based on the use of wave characteristics; attenuation and dispersion in phase velocity. To achieve this goal, a multi-channel test configuration is implemented at ultrasonic frequency range and the recorded signals are subjected to advanced signal processing techniques to extract the most relevant information. The investigations are completed in two phases. In the initial phase, the methodology is developed on a half-space medium of lightly cemented sand. The soft cemented-sand specimen is damaged by drilling regular-shaped holes along the area

under investigation. The ultrasonic tests are repeated for different depths of holes to study the sensitivity of the wave characteristics (attenuation and dispersion) with respect to the damage depth. Wave attenuation is determined by utilizing discrete wavelet transform while the dispersion in phase velocities is extracted from two-dimensional Fourier transform. A new index representing the cumulative variation in the phase velocity with respect to the reference dispersion curve obtained from the intact material is defined to evaluate the condition of the discrete defects in a quantitative manner. Following the study on the regularly shaped defects, the second phase is conducted on six laboratory-scale concrete beams with different levels of aggregates in order to evaluate the damage level of the unevenly distributed defects to show the potential of the new methodology to identify distributed damage in concrete members.

2 THE ASSESSMENT METHODOLOGY

2.1 Surface Wave Attenuation

Dissipation of wave energy occurs due to geometric radiation and material damping. The former caused by increasing surface area of a propagating wave, whereas the latter is related to heat, inelastic deformations, and friction. The spatial attenuation coefficient α_x for a propagating wave is defined as $\alpha_x = \frac{1}{x_2 - x_1}\left[\ln\left(\frac{A_2}{A_1}\right) - \beta \ln\left(\frac{x_2}{x_1}\right)\right]$ (Richart et al. 1970), where A_1 and A_2 are the amplitudes at distance x_1 and x_2 from the source, and β is the geometric attenuation constant which is equal to -0.5 for surface waves (cylindrical wave-front). Different signal processing techniques can be used to compute the coefficient α_x. In this study, discrete wavelet transform (DWT) is preferred as it is demonstrated by Kirlangic et al. (2015) as a reliable and convenient method to determine the attenuation of the interested frequency range. The discrete wavelet transform is advantageous over the conventional Fourier transform since it provides the temporal information for the interested frequencies by decomposing a time signal into its sub-signals of each is associated with a specific frequency band-width (Addison, 2002).

2.2 Dispersion of Phase Velocity

Wave propagation in a bounded medium is complicated due to multiple reflections of waves between the boundary surfaces and mode conversions of body waves. In the case of a plate, the interaction of waves generates Lamb modes as defined with the Rayleigh-Lamb frequency equation (Graff, 1975). The Lamb modes are frequency dependent, in other words dispersive. However, at high frequencies they are considered as Rayleigh waves travelling at constant velocity since the wavelengths become shorter compared to the medium thickness. The R-wave velocity V_R depends only on the dilatational and distortional wave velocities, which are governed by the elastic properties.

In practice, the dispersion in wave propagation is investigated by utilizing a test configuration comprising multiple receivers to acquire time signals simultaneously at different locations. The two-dimensional Fourier transform (2D FT) of these recorded signals provides a two-dimensional spectrum in frequency-wavenumber domain which is called f-k plot. To avoid spatial aliasing in the plot, the interested frequency should have at least a wavelength λ equal to the receiver spacing Δx (Heisey et al. 1982). The f-k plot allows the identification of incident, reflected and transmitted events in frequency-wavenumber domain, so that the phase velocities (i.e. dispersion curve) of each event can be computed simply by extracting the peaks appeared in the plot. In the case of a homogeneous half-space, the dispersion curve is a straight line of

which slope represents the V_R. However, any disruption in the phase velocity due to any type of anomaly appears in the f-k plot which can be used to interpret the damage condition.

3 EXPERIMENTAL METHODOLOGY

Experimental works are conducted in two phases: in the first phase the methodology is established on the regularly shaped defects in a half-space medium made of cement-sand mixture, whereas in the latter phase the randomly distributed irregular defects in concrete beams are investigated.

3.1 Experimental Work Phase I: Regular Defects in Half-space Medium

3.1.1 Laboratory Setup and Test Configurations

The proposed damage assessment methodology is developed on a medium made of cement and sand. The test medium is made of Silica sand (Barco #71) mixed with 10% gypsum cement by weight. The particle size distribution of the sand is given as D_{10} = 0.12 mm, D_{50} = 0.18 mm, C_u = 1.8, and C_c = 1.04 (Khan et al. 2004). The specimen has a depth of 30 cm with horizontal dimensions of 106 and 87 cm. The medium represents a half-space medium with the given dimensions and boundary conditions for the ultrasonic wavelengths used in this study. The cemented-sand is preferred in order to induce damage easily. A drill with a 6.35 mm bit is used to create vertical holes within the medium. The damaged section is created at the center of the receiver array, 21.75 cm away from the source transmitter (Fig. 1a). The chosen distance between the damaged zone and the transmitter allows wavelengths up to 21 cm to form before encountering the defects shown in Figure 1b. This distance provides the ability to investigate frequencies as low as 6.5 kHz. The hole depth is increased up to 12 cm with 1 cm increment. After each increment in depth, the ultrasonic test is repeated. The total number of the ultrasonic tests performed is 13 including the non-damaged case. The receivers are not moved until the last test is completed. Each test data is named after the hole depth (e.g. D05 represents the case of 7 holes with 5 cm depth).

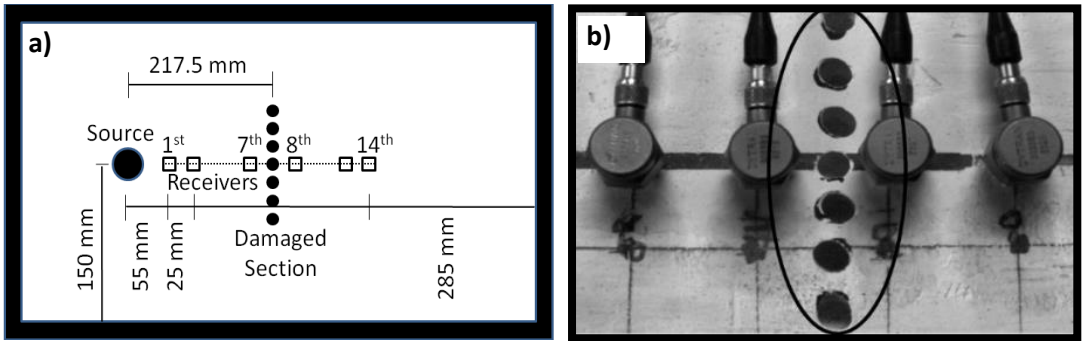

Figure 1. (a) Testing configuration (Not to scale) (b) the damaged section on the rigth.

The test instrumentation includes an ultrasonic piezoelectric transmitter (resonant frequency of 50 kHz) driven by a piezo-driver. 14 piezoelectric accelerometers (Dytran 3055B3, flat frequency range of 1-10,000 Hz, nominal resonant frequency above 35 kHz, power supplied by PCB 483) are used to capture the signals. The signals are recorded using a 24-channel high frequency data acquisition system (LDS Nicolet Genesis).

3.1.2 Data Analysis: Attenuation

After eliminating the geometrical attenuation in time histories, the spatial attenuation coefficient is calculated based on the spectral area of the decomposed signals from DWT. The attenuation trend is fitted to $e^{\alpha_x(x_1-x_i)}$ in order to estimate the coefficient α_x, where x_i is the location of the receiver respect to the source. The decomposition of the signals in DWT is performed by employing the Daubechies wavelet d18 (Addison, 2002), which is preferred due to its similarity with the measured signal. The sub-signal associated with the frequency bandwidth of 31.25 - 62.5 kHz provides an attenuation trend with the highest coefficient of determination R^2 with 0.85 among all the sub-signals since its frequency range contains most of the spectral energy supplied by the transmitter. The normalized attenuation trend for the non-damaged case shown in Figure 2a is obtained from the signals windowed by Tukey windows.

The spatial attenuation coefficient calculated for each damage case, plotted in Figure 2b, justifies the correlation between the attenuation and the defect depth. The coefficient α_x increases up to 24% of its initial value at case D08, and then loses its sensitivity to damage beyond that by converging to a constant value. Thus beyond this depth, larger wavelengths should be investigated by employing transmitters capable of generating lower frequencies.

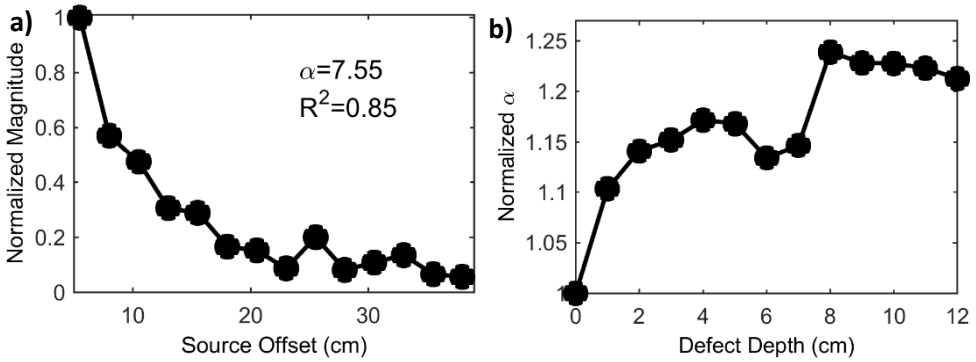

Figure 2. (a) Attenuation trends (case D00), (b) the α computed for each damage case.

3.1.3 Data Analysis: Dispersion in Phase Velocity

The experimental dispersion curves are extracted from the frequency-wavenumber plots, which are generated by performing the 2D Fourier transform of 14 measured signals. The same windows used in the attenuation calculations is employed prior to the 2D FT, so that the ripples observed in the f-k plot of the non-windowed signals are eliminated and the frequencies carrying major energy are exposed. By selecting the frequencies and the wave-numbers associated with the maximum magnitudes of the 2D spectrum, the phase velocities V_{ph}, constituting the dispersion curve displayed in Figure 3a, are calculated. The curve exhibits the first anti-symmetrical Lamb mode (the flexural mode) clearly for the lower frequencies, whereas it converges to a constant R-wave velocity at around 1200 m/s as the frequency increases. The dispersion of the lower frequencies is caused by the relatively short thickness of the cemented-sand. Given the fact that the vertical excitation is induced by the transmitter, the existence of the flexural modes is expected for the low frequencies.

The experimental dispersion curves are used to determine the dispersion index *DI* which represents the correlation between the dispersion in phase velocity and the damage depth. The phase velocities for the intact case (D00) given in Figure 3a is curve-fitted to provide continuity in the reference dispersion curve for the frequency range of 0 to 50 kHz. After inducing 1 cm damage depth (D01), a new dispersive behavior is observed for higher frequencies in the curve,

which grows with the increasing damage depth. In other words, as the damage extends, broader range of frequencies contributes to dispersion as shown for some of the selected cases in Figure 3a. The dispersion index is defined as $DI^{\langle case \rangle} = \sum \Delta V_{ph}^{\langle case \rangle}(f)/V_{ph}^{\langle 0 \rangle}(f)$, where $\Delta V_{ph}^{\langle case \rangle}(f) = \left| V_{ph}^{\langle case \rangle}(f) - V_{ph}^{\langle 0 \rangle}(f) \right|$. The *DI* is the summation of variations in the phase velocity normalized with regard to the reference phase velocity from case D00. This calculation is performed for each frequency within the specified bandwidth. The dimensionless *DI* summarizes the variation of phase velocities into one single index which makes it easier to quantify the damage. The dispersion index calculated for each damage depth is plotted in Figure 3b. The change in the *DI* between damage cases D01 and D12 is 51% which makes it more sensitive to damage compared to the coefficient α_x whilst the R^2 found as 0.92 indicates moderate linear correlation of the index with the damage depth. Similar to the α_x, the *DI* does not reveal meaningful sensitivity beyond 7 cm damage depth confirming the insufficiency of the transmitter beyond this depth.

The investigations in the first phase of the experimental works result in the signal processing procedure shown in Figure 4 which is also implemented in the second phase of this study on the concrete beams as explained next.

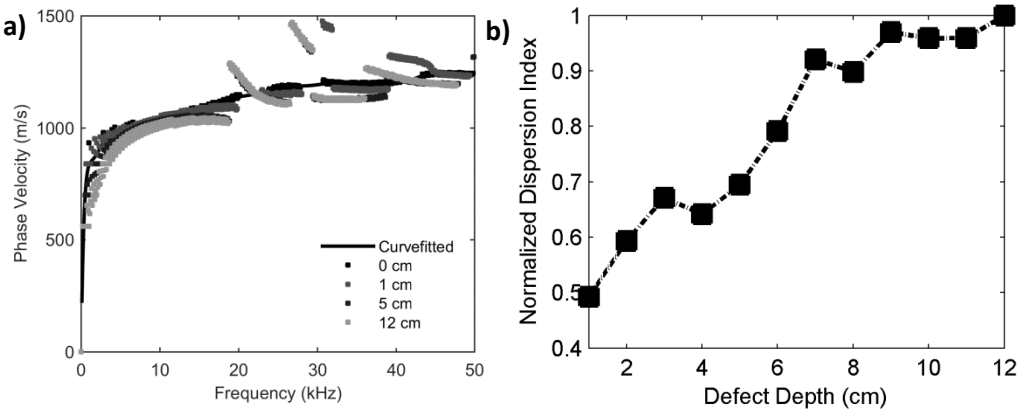

Figure 3. (a) Dispersion curves for case D00, D01, D05, D12 (b) Dispersion index vs. damage case.

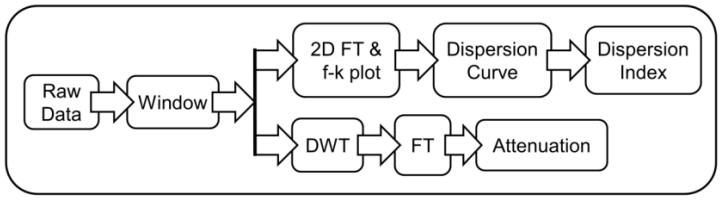

Figure 4. Signal processing algorithm.

3.2 Experimental Work Phase II: Irregular Defects in Concrete Beams

3.2.1 Laboratory Setup and Test Configurations

In the second phase, the assessment procedure (Fig. 4) developed on the half-space medium with regular defects is implemented on concrete beams with irregular defects. Ultrasonic and mechanical tests are conducted on six laboratory-scale concrete beams (110x15x10 cm^3), each having a different void percent. The voids are created by mixing the concrete paste with spherical Styrofoam pellets of 7 mm diameter. The beams contain 0%, 5%, 10%, 15%, 20% and 30% pellets in volume and each one is named after its defect volume (e.g. B05 denotes the beam containing 5% pellets in volume). Concrete batches are produced by mixing Type I Portland

cement with coarse aggregate (D_{max}=9.5 mm) and sand in a machine mixer without any additive. The water-cement ratio is kept 0.6 for all beams. During casting of the fresh concrete, no vibrator is employed to prevent the pellets from rising towards to the surface of the wet concrete. The beams are kept in the humidity room for 28 days.

The ultrasonic test setup consists of the same instrumentation used on the cemented-sand earlier; however, this time a set of 18 accelerometers is employed. All receivers are fixed at once along the center line of the beam under test. The transmitter is located 30 cm away from the beam edge while the receiver spacing and the source offset to the first receiver is 2 and 6 cm respectively.

Following the ultrasonic tests, the beams are cut into five prisms (10x15x10 cm^3) in order to visually control the pellet distribution in the beams. Apart from the pellets, air voids are also observed in the cross-sections. Apparently the real void volumes are larger than the intended ones due to the poor compaction. However, the compressive strengths of the beam sections, which are measured in accordance with CSA A23.2-9C, reveal a linear reverse correlation with the intended void volume (Fig. 5a) justifying that the real defect volume is in accordance with the intended ones in general. The average compressive strength drops around from 45 to 10 MPa with increasing void volume. The initial %5 void causes approximately 20% drop in strength, whereas the beams with 15% and 20% void have approximately same strength. This can be attributed to the fact that the real void volume does not differ meaningfully between the investigated sections of these two beams.

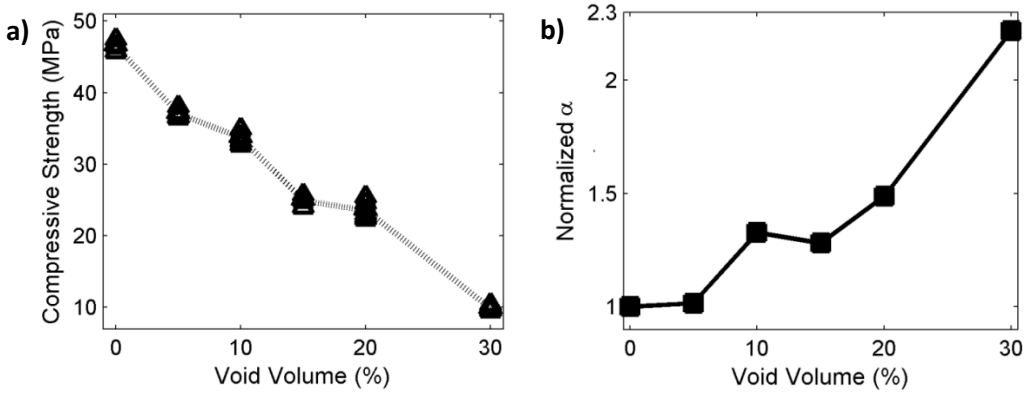

Figure 5. (a) Compressive strength of the beam sections (b) the attenuation coefficient

3.2.2 Data Analysis: Attenuation

The R-wave is found as 2384 m/s and 1624 m/s for B00 and B30 respectively based on the arrival times as shown in Figure 6. Further the receiver from the source, larger amplitudes in time histories are observed later than the arrival of the wave-front which indicates the constructive behavior of the incident and the reflected events. Therefore, each signal is windowed by a Tukey window whose length is set in accordance with the expected arrival time of the reflection. Thus the attenuation is determined mostly based on the incident event by minimizing the effect of the reflections.

The attenuation coefficient of the concrete beams is determined by the DWT as discussed in the first phase. However, this time the geometric attenuation is not eliminated from the original signals as the attenuation in concrete is less significant compared to the cemented-sand. Instead, the total attenuation coefficient α, which represents the combined material and geometric attenuation, is preferred. The coefficient α indicates high sensitivity with 120% increase respect

to its initial value for 30% void as displayed in Figure 5b. Although, B15 does not fit the trend, the overall increase in attenuation is apparent with the increasing void volume.

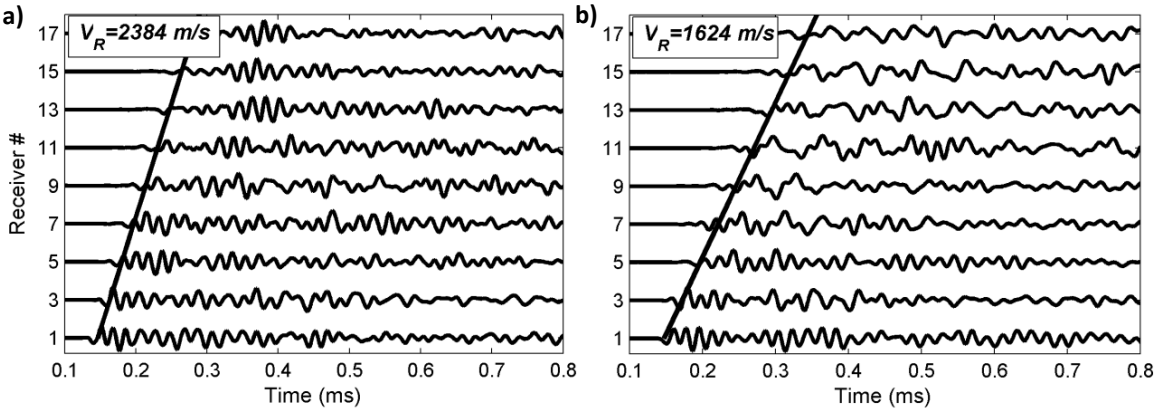

Figure 6. Time histories for (a) B00 and (b) B30.

3.2.3 Data Analysis: Dispersion in Phase Velocity

The procedure introduced in the first phase is pursued for the concrete beams as well. The same window sizes used for the calculation of the coefficient α are applied to the signals prior to the 2D Fourier transform in order to extract the incident waves. Then the phase velocities are determined from the f-k plots (shown for B00 and B30 in Figure 7) where the effect of the defects on the dispersion is observed clearly. The reference dispersion curve obtained from B00 is curve-fitted up to 120 kHz as being the maximum frequency for Δx=2 cm without spatial aliasing for V_R=2384 m/s.

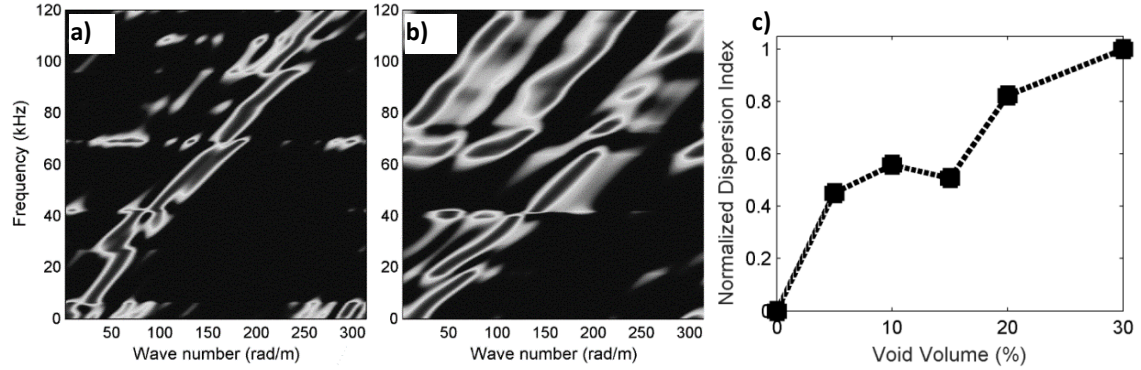

Figure 7. The f-k plot for (a) B00 and (b) B30, (c) the dispersion index vs. void volume.

The trend of the DI displayed in Figure 7c is in agreement with the results for the attenuation; similarly B15 does not follow the trend. The change in the DI between B05 and B30 is almost %100 which makes it almost as sensitive as the attenuation coefficient. In the case of a surface breaking notch or delamination in the concrete, existence of the Lamb modes could be tracked to detect the defect; however, when the voids distributed all over the beams, it is hard to observe any clear mode conversion. Nevertheless, the defects are still capable of disturbing the R-wave travelling with a constant velocity depending on their size and location. Therefore, the dispersion index is a promising feature to quantify the defect volume.

4 CONCLUSIONS

The developed condition assessment procedure for cemented materials based on attenuation and dispersion in the ultrasonic frequency range is presented. The discrete wavelet transform is used to determine the frequency dependent attenuation whereas a new diagnostic feature, the dispersion index, is defined based on the relative dispersion occurred due to the defects. Based on the knowledge attained on the regularly shaped defects, the assessment procedure is implemented on the concrete beams with irregular defects. Despite the complex structure of the defect patterns and beam geometry, promising results are obtained for both attenuation and dispersion based assessments. In the future, the pilot study on the beams is to be extended to the beams with more intermediate defect volume in order to validate the correlations between the wave characteristics and the defect content. The proposed procedure is applicable to other construction materials such as rocks, and pavements as long as effective frequency range is excited and appropriate testing configuration (i.e. source offset and receiver spacing) is implemented.

5 REFERENCES

Addison, P., 2002, *The Illustrated Wavelet Transform Handbook: Introductory Theory and Applications in* Science, Institute of Physics Publishing, Bristol and Philadelphia.

Aggelis, D. G., and Shiotania, T., 2007, "Experimental Study of Surface Wave Propagation in Strongly Heterogeneous Media," *Acoustical Society of America*, Vol. 122, No. 5, pp. 151-157.

Aggelis, D. G., 2009, "Numerical Simulation of Surface Wave Propagation in Material with Inhomogeneity: Inclusion Size Effect," *NDT and E International*, Vol. 42 No. 6, pp. 558-563.

Aggelis, D. G., and Momoki, S., 2009, "Numerical Simulation of Wave Propagation in Mortar with Inhomogeneities," *ACI Materials Journal*, Vol. 106, No. 1, pp. 59-63.

CSA A23.2-9C, 2009, Compressive Strength of Cylindrical Concrete Specimens, Canadian Standards Association.

Graff, K. F., 1975, Wave motion in elastic solids, Ohio State University Press, Belfast.

Heisey, J. S., Stokoe, K. H., Hudson, W. R., and Meyer, A. H., 1982, *Research Report 256-2: Determination of in situ wave velocities from spectral analysis of surface wave*, University of Texas: Centre for Transportation Research, Austin.

Kalinski, M. E., Stokoe, K. H., Jirsa, J. O., and Roesset, J. M., 1994, "Nondestructive identification of internally damaged areas of concrete beam using the SASW method," *Transportation Research Record*, Issue 1458, pp. 14-19.

Khan, Z., Majid, A., and Cascante, G., 2004, "Measurement of ultrasonic wave velocities," *Canadian Geotechnical Society*, Quebec city, Quebec, October 2004, Canada.

Kirlangic, A. S., Cascante, C., Polak, M., 2015, "Condition Assessment of Cementitious Materials Using Surface Waves in Ultrasonic Frequency Range," *ASTM International Geotechnical Testing Journal*, Vol. 38, No. 2, pp. 1-11.

Popovics, J. S., & Song, W. J., 2000, "Application of surface wave transmission measurements for crack depth determination in concrete," *ACI Materials Journal*, Vol. 97, No. 2, pp. 127-135.

Richart, F.E. Jr., Hall, J.R. and Woods, R.D., 1970, *Vibrations of Soil and foundations.* Prentice-Hall, Englewood Cliffs, New Jersey.

Yang, Y., Cascante, G., and Polak, M., 2009, "Depth detection of surface-breaking cracks in concrete plates using fundamental Lamb modes," *NDT & E International*, Vol. 42, No. 6, pp. 501-512.

Zerwer, A., Polak, M., and Santamarina, J. C., 2003, "Rayleigh Wave Propagation for the Detection of Near Surface Discontinuities: Finite Element Study," *Journal of Nondestructive Evaluation*, Vol. 22, No. 2, pp. 39-52.

Zerwer, A., Polak, M., and Santamarina, J. C., 2005, "Detection of surface breaking cracks in concrete members using Rayleigh waves," *Journal of Environmental & Engineering Geophysics*, Vol. 10, No. 3, pp. 295-306.